Eighth Australasian Fluid Mechanics
Conference, University of Newcastle,
N.S.W., 28 November/2 December 1983.

THE EFFECTS OF STREAMLINE CURVATURE ON THE REATTACHING TURBULENT FLOW OVER A BACKWARD-FACING STEP

S. HONAMI AND I. NAKAJO

DEPARTMENT OF MECHANICAL ENGINEERING

UNIVERSITY OF TOKYO, SHINJUKU, TOKYO 162 JAPAN

SUMMARY The paper presents the behavior of a separating shear layer and its reattachment when an additional centrifugal body force due to streamline curvature is imposed on the shear layer. A curved channel is attached to a backward-facing step to obtain such a flow situation. In addition to the inherent stability within the conventional straight channel, the stabilizing and destabilizing effects on the reattachment process are given according to the direction of curvature. Three different surface configurations are used (flat, convex, and concave); with weak and mild surface curvature, the measurements were performed for five separate cases. The reattachment point was determined by a wall-flow direction probe based on a heat tracer method. Flow visualization of the shear layer was made by means of a smoke-wire method. Reynolds number based on step height was 8×10^4, curvature parameter being in the range $-0.022 < \delta/R < 0.026$.

NOMENCLATURE

Cf/2	Skin friction coefficient
Cp	Pressure coefficient, (P-Pref) / (1/2)ρUref^2
Er	Expansion ratio, h2/h1
H12	Shape factor
H	Step height (= 40 mm)
h1	Channel height upstream of step (= 80 mm)
h2	Channel height downstream of step (= 120 mm)
P	Wall static pressure
R	Radius of surface curvature
ReH	Reynolds number based on step height
Reθ	Reynolds number based on momentum thickness
u´	Turbulence intensity
U	Streamwise velocity
x	Streamwise distance from step base
Xr	Reattachment length
Xs	Reseparation distance from step base
W	Channel width (= 720 mm)
γ_p	Time fraction of downstream flow
δ	Boundary layer thickness
θ	Momentum thickness
ρ	Density (air)

Subscript

ref	Refernce point, x = -150 mm
w	Wall

INTRODUCTION

The backward-facing step flow has been an important subject of concern. A comprehensive review of the numerous literatures was given by Bradshaw (1972) and Eaton (1981). The various effects on the reattachment and the recovery process have been discussed.

In spite of many previous works, our understanding of the stability effect due to streamline curvaure in the separating shear layer has not reached the explicit conclusion. The radius of dividing streamline curvature was estimated to be an order of 10 step heights near the reattachment point by Eaton (1980), while 50 step heights after the step. It is difficult to explain how the stabilizing effects suppress the Reynolds stress in the shear layer and even in the reattached boundary layer.

Knowledge on the stability in the backward-facing step flow is improved if additional streamline curvature is imposed on the separating shear layer in the recirculating and the reattachment zone. In order to obtain such a flow situation, a two-dimensional curved channel is attached to a backward-facing step. Of course, the shear layer after separation in the conventional straight channel corresponds to the stable one in the sense of stability. In addition to the inherent stability, the stabilizing or destabilizing effects on the reattachment process are given according to the direction of surface curvature. Three kinds of surface geometry and two kinds of surface curvature are used as the test conditions in the present experiment. A curvature parameter is in the range $-0.022 < \delta/R < 0.026$. Therefore, the effects of additional streamwise curvature on the behaviors of separating shear layer and the reattachment process are clarified.

The attention was paied to the upstream condition for the experiment. Since the fully developed turbulent boundary layer was provided at the step, the Reynolds number based on the momentum thickness was an order of 4600, above the value for a laminar to turbulent flow transition. The nondimensional boundary layer thickness, δ/H, amounts to an order of 0.5. Therefore, the low Reynolds number effect on the reattachment process is avoid.

APPARATUS AND TECHNIQUES

Fig. 1 shows a schematic of the test geometry used. The air flow tunnel is an open-return type. A flow straightener with a honeycomb section, six screens, and a two-dimensional 10-to-1 contraction nozzle are set at the inlet section. The test channel is a 1500 mm straight development section and a curved test section, and the length of the test section is about 2000 mm. A backward-facing step corresponds to the edge at the end of the straight development section, since an expansion

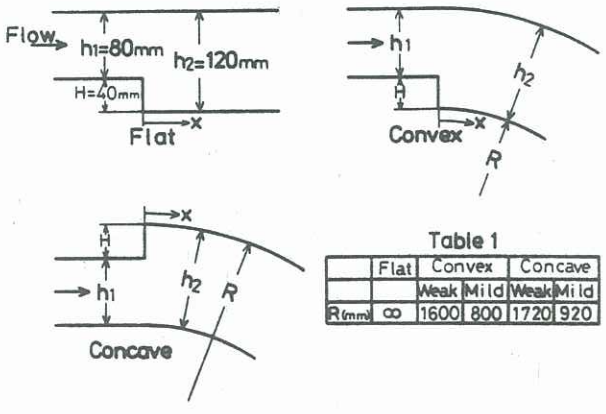

Table 1

	Flat	Convex		Concave	
		Weak	Mild	Weak	Mild
R(mm)	∞	1600	800	1720	920

Figure 1 Test section schematic

Table 2 Boundary Layer Parameters (reference point)

Geometry / Curvature	Flat	Convex Weak	Convex Mild	Concave Weak	Concave Mild
δ mm	20.9	21.8	20.4	20.6	20.5
θ mm	2.37	2.48	2.39	2.35	2.34
H12	1.38	1.38	1.39	1.39	1.39
Cf/2	0.00153	0.00152	0.00154	0.00151	0.00154

ratio of test section height to upstream straight section height (= h2/h1) is 1.5. A tripping plate 1.5 mm x 1.5 mm in cross section is attached at the nozzle throat. Table 1 shows the channel dimension of the test geomtry. Three different surface configurations are used (flat, convex, and concave); with two kinds of weak and mild surface curvature, the measurements are made for all the five cases. While no attempt was made to minimize the secondary flow created by end-wall flow, the use of a large aspect ratio kept secondary flow effects small, the ratio of channel width W to height h2 being 6. The ratio of channel width to step height is 18-to-1.

Pressure taps 0.5 mm in diameter were installed at 20 mm interval along the centerline of the test wall. The pressure gradient was obtained from the measured wall static pressure distributions by using a cubic-spline data-smoothing program. Mean velocity profiles on the center and the off-centerline at the reference point 3.75 step heights upstream of the step edge were measured with a Pitot-tube. Detailed boundary layer parameters at the reference point are given in Table 2. The spanwise uniformity of the flow upstream of the step was checked. The momentum thickness distributions show the change within 4 % over the central 70 % of the development section. A turbulence data was also acquired at the reference point using a hot-wire anemometer which was a linearized constant temperature type. The turbulence intensity in the free stream is an order of 0.2 % for each of the five cases. The Reynolds number based on momentum thickness at the reference point (x = -150 mm), Re_θ , is 4600, except for the experiment on the low Reynolds number effect. The step height Reynolds number ReH is $7.7\text{-}8.1 \times 10^4$.

The wall-flow direction probe flush-mounted on the wall indicates the instantaneous flow direction in the vicinity of the test surface. The electronic circuit designed by Eaton (1979) was improved to diminish the level of the noise and the drift. A time fraction of downstream flow, γ_p, was determined by averaging during 128 seconds by an integral voltmeter with a volt-frequency converter. The values of γ_p measured in both orientations were averaged, where the wire height was 1 mm from the wall. The reattachment point was defined as the location of the 50 % downstream flow point in the reattachment by Eaton (1980).

The smoke wire technique for flow visualization was employed to obtain a frozen picture of an unsteady flow within the shear layer and near the reattachment point. The smoke wire was installed in the spanwise direction to observe the spanwise non-uniformity due to separation and reattachment process.

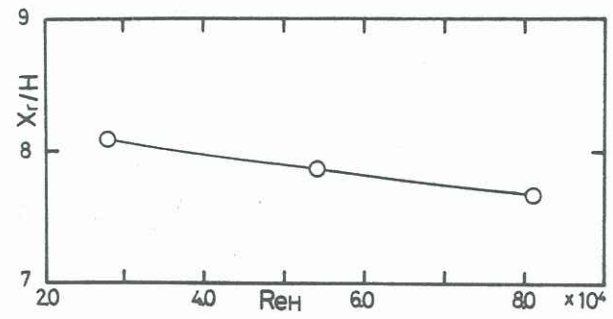

Figure 2 Mean reattachment length for different Reynolds number (flat surface)

RESULTS AND DISCUSSIONS

Fig. 2 shows the results of the upstream condition on the mean reattachment length in the case of the flat surface of the test section for different Reynolds numbers which was varied by changing the tunnel velocity. The reattachment length was determined by means of the wall-flow direction probe. Durst (1983) demonstrated that the parameter ReH played a significant role in the mean velocity field. A laminar to turbulent transition occurred at $ReH = 0.5 \times 10^4$. The change in Xr/H was not sensitive to the Reynolds number above 3×10^4. A comparison of the measured reattachment length indicates the same trend as the results by Durst (1983). Then, a series of experimental results which will be discussed for the five cases was performed in the highest Reynolds number range.

Fig. 3 shows the wall static pressure measurements for the five cases. The pressure distribution for the flat case has the same characteristics as in many previous experiments. Although the rapid increase in pressure coefficient occurs similarly in the reattachment zone, the wall static pressure distributions up to about x/H = 0.5 in the recirculating zone have the different features among the all cases. The cause of this difference may be related to pressure difference in the radial direction due to test channel curvature, resulting in the different behavior on reseparation in the recirculating zone. The pressure rise in the reattachment zone will be discussed later.

Fig. 4 indicates the near-wall distributions of the time fraction of downstream flow, γ_p, for the five separate cases. Each reattachment length is also given in Fig. 4. The result for the flat case is reasonably consistent with the data by Durst (1983) in comparison with the expansion ratio and the Reynolds number. Since the distribution of γ_p shows the similar trend in all five cases, a weak dependence of surface geometry and curvature on the reattachment length was observed in the present series of data. In contrast, the reattachment length in an angled backward-facing step flow measured by Westphal (1982) is linearly proportional to the deflection angle of the test channel.

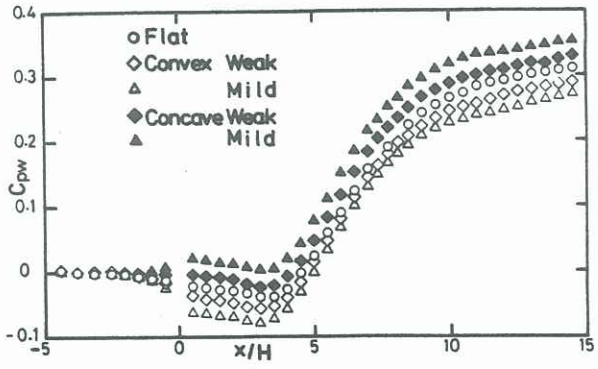

Figure 3 Wall static pressure distributions

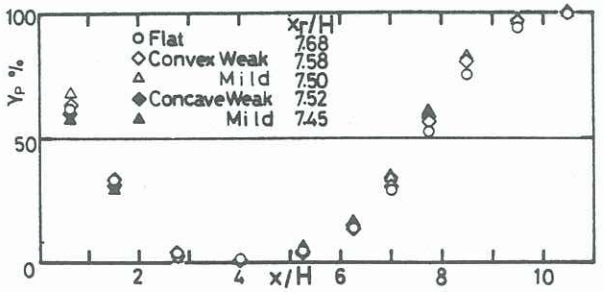

Figure 4 Time fraction of downstream flow

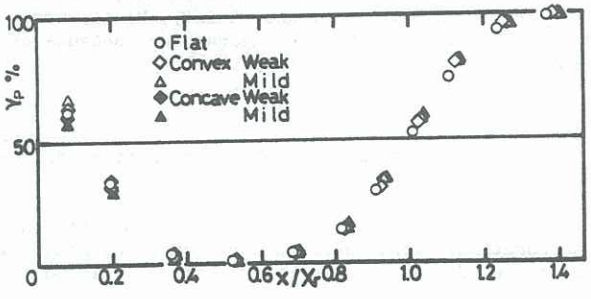

Figure 5 Time fraction of downstream flow vs. streamwise distance scaled on reattachment length

Fig. 5 depicts the γ_p distributions plotted versus streamwise distance normalized by the reattachment length for each of the five cases. The similar relation was obtained in the region above x/Xr = 0.4. The coincidence is believed to be caused by the similarity on the near-wall flow. The reseparation in the recirculating zone, however, occurs at the different location near the step, because of the different pressure gradient in both the streamwise and radial (normal to the wall) directions as mentioned before (Fig. 3).

Eaton (1980) estimated the radius of dividing streamline curvature from the mean velocity measurement in case of the flat surface. The streamline radius of curvature is about 50 step heights in the recirculating zone upstream of x/H = 4, while it is an order of 10 step heights near the reattachment zone. The shear layers in these two zones are about or more than one step height thick, respectively. Therefore, the additional effect of the radius of surface curvature on the shear layer is expected to be strong upstream of x/H = 4, since the radius of mild or weak curvature used in the experiment is in the range of about 20 or 40 step heights. On the other hand, additional streamline curvature may have little effect on the shear layer structure in the reattachment zone, especially near the wall region.

Fig. 6 also shows the static pressure distributions where Cpw min means a minimum value of Cpw in the recirculating zone,i.e., a base pressure coefficient. The similar pressure rise for the five cases is found in the reattachment zone, except very close to the step base and further downstream of the reattachment point, when scaled on the reattachment length. Despite the different flow history due to the variations in channel geometry, the near-wall flow has the similar characteristics among all the five cases.

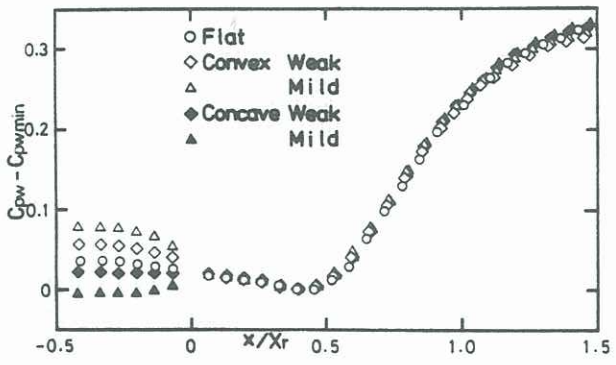

Figure 6 Static pressure rise vs. streamwise distance scaled on reattachment length

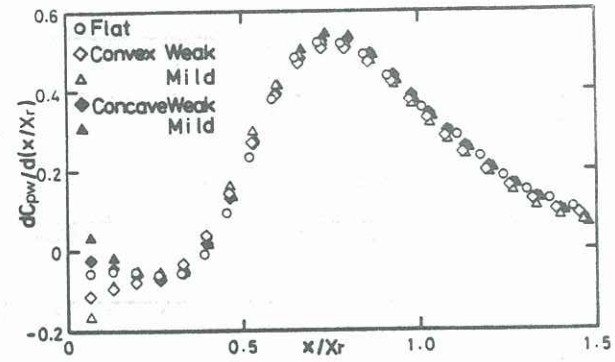

Figure 7 Pressure gradient vs. streamwise distance scaled on reattachment length

Fig. 7 shows the pressure gradient in the streamwise direction for each of the five cases, where Xp is defined as the streamwise location which indicates the peak pressure gradient. The noticeable feature is that the peak pressure gradient for the cases with zero or stabilizing curvature occurs at the location near x/Xr = 0.75,i.e., Xp = 0.75 Xr, while the location of the peak for the concave cases somewhat moves towards downstream. This difference may be related to the different structures on the shear layer due to the stabilizing and destabilizing effects, although the difference seems small. The shear layer with destabilizing curvature appears to have the much complicated history up to the reattachment point, since it may be influenced by the remarkable stabilizing effect with approaching the reattachment point after the mild (weak) destabilizing effect happens; the radius of dividing streamline curvature roughly changes from -20H (-40H) to about 10H in the case of mild (weak) concave curvature. The pressure rise in the reattachment zone strongly depends on the expansion ratio, nevertheless the spanwise length indicating the peak pressure gradient, Xp, is independently about 75 % of the reattachment length. In spite of the various expansion ratio and the initial conditions, the similar trend was also obtained from the data by Chandrsuda (1975) and Eaton (1980).

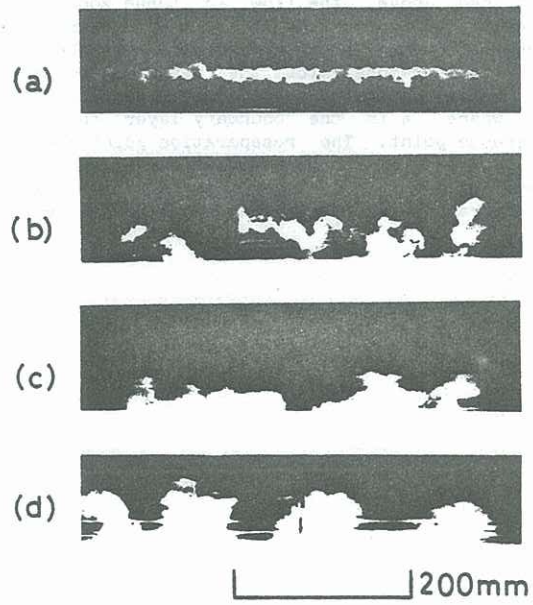

Figure 8 Shear layer behavior by flow visualization
(a) After separation for flat surface case, x/H=4
(b) After reattachment for flat surface case, x/H=8.5
(c) After reattachment for mild convex case, x/H=8.75
(d) After reattachment for mild concave case, x/H=8.75

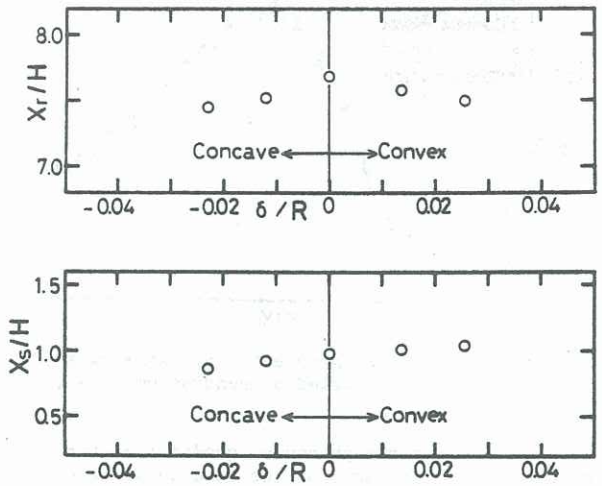

Figure 9 Reattachment length and Reseparation point vs. curvature parameter

Eaton (1980) checked the spanwise uniformity of the flow in the reattachment zone by the wall-flow direction probe measurements. The reattachment line seems very straight in the sense of long time averaged measurements. Fig. 8 shows the spanwise behavior of the shear layer over the central 70 % of the channel width near the step and after the reattachemnt point with the smoke-wire technique. The photograph was taken to obtain a frozen picture of the flow by the use of the strobo with a short duration time less than hundred micro-seconds. The delay time between the smoke generation and strobo flash was about 20-30 mili-seconds. The smoke after the step uniformly distributes in the spanwise direction as shown in Fig. 8 (a). The discrete smoke lumps downstream of the reattachment point, however, were observed in the spanwise direction, especially in the case of mild concave curvature. These smoke agglomerations may be caused by both the shear layer characteristics and the tunnel surface configuration, like surface curvature, in the reattachment and the recovery zone. In contrast to the long time averaged results by the wall-flow direction probe as mentioned above, the flow in these zones shows the spanwise non-uniformity from the results of a large number of photograghes taken for each of the five cases.

Fig. 9 demonstrates the mean reattachment length and the reseparation point for the curvature parameter, δ/R, where δ is the boundary layer thickness at the reference point. The reseparation point was defined as the location of the 50 % downstream flow point near the step base. Small dependence of the test surface configuration on the mean reattachment length Xr is found in the curvature range examined. The reseparation in the recirculating zone, however, indicates the somewhat universal behavior. Although the reseparation distance Xs involves some uncertainty, Xs appears to be proportional to the curvature parameter because of the pressure gradient near the step base.

CONCLUSION

The main conclusions obtained in five different test cases are as follows.

1 The reattachment length Xr depends on the channel configuration, like surface curvature, although weak dependence of the curvature parameter δ/R is obtained.

2 Both the static pressure and the time fraction of the downstream flow γp show the similar distributions, when streamwise location is scaled on the reattachment length.

3 Peak pressure gradient occurs at the 75 % of the reattachment length among the cases.

4 The flow after the reattachment point shows the spanwise non-uniformity from flow visualization.

The authors wish to thank Messrs M. Uematsu, Y. Noguchi, W. Ito and Y. Oguchi who assisted in the test facility construction and data acquisition.

REFERENCES

Bradshaw, P. and Wong, F. Y. F. (1972) The Reattachment and Relaxation of a Turbulent Shear Layer. J. Fluid Mech., 52, 113-135.

Chandrsuda, C. and Bradshaw, P. (1981) Turbulence Structure of a Reattaching Mixing Layer. J. Fluid Mech., 110, 171-194.

Eaton, J. K. et al. (1979) A wall-Flow Direction Probe for Use in Separating and Reattaching Flows. Trans. ASME J. Fluids Engrg, 101, 364-366.

Eaton, J. K. and Johnston, J. P. (1980) Turbulent Flow Reattachment: An Experimental Study of the Flow and Structure behind a Backward-Facing Step. Stanford University ,MD-39.

Eaton, J. K. and Johnston, J. P. (1981) A Review of Research on Subsonic Turbulent Flow Reattachment. AIAA J, 19, 1092-1100.

Durst, F. and Tropea, C. (1983) Structure of Complex Turbulent Shear Flow, Springer-Verlag, 41-52, Springer.

Westphal, R. V. and Johnston, J. P. (1982) 1980-81 Stanford Conference on Complex Turbulent Flows, Vol 2: Predictive case P3, Stanford Univ., 902-904.